Expected nucleation effects of carboxylic acid salts on poly(1-butene)

Tao Zheng[1], Qian Li[2], Qian Zhou[1], Huayi Li[2*], Qian Xing[1*], Liaoyun Zhang[1], Youliang Hu[2]

[1] College of Chemistry and Chemical Engineering, University of Chinese Academy of Sciences, Beijing 100049, China

[2] Beijing National Laboratory for Molecular Sciences, CAS Key Laboratory of Engineering Plastics, Institute of Chemistry, Chinese Academy of Sciences, Beijing 100190, China

ABSTRACT

9,10-Dihydro-9,10-ethano-anthracene-11,12-dicarboxylic acid disodium salt (DHEAS) was synthesized and used as a nucleating agent for poly(1-butene) (iPB). The isothermal crystallization kinetics of iPB having different nucleating agents were investigated by differential scanning calorimetry (DSC) and polarized optical microscopy (POM). The results showed that the nucleating agents increased the crystallization temperature and the crystallization rate and shortened the crystallization half-time ($t_{1/2}$). As well, the nucleating agents could be used as heterogeneous nuclei in the iPB matrix and decreased the size of iPB. When the nucleating agent was DHEAS, the crystallization temperature of iPB was up to 93.6°C which was higher than that of other nucleating agents for iPB and pure iPB. The crystallization half-time in the presence of DHEAS was 0.58 min which was less than that of other nucleating agents for iPB and pure iPB. In this case, the spherulitic size of iPB was the smallest and the morphology was changed, which indicated that DHEAS displayed better nucleation effect among the studied nucleating agents. **Polyolefins J 3:37-45**

Keywords: Nucleating agent; DHEAS; poly(1-butene); polarized optical microscope; crystallization half-time

INTRODUCTION

Poly(1-butene) (iPB) has wide applications in many fields due to its good heat-resistant creep degeneration, good environmental stress cracking resistance performance, and good tenacity [1-4]. The structure and morphology of iPB have a direct impact on the crystallization behavior which ultimately affects the final mechanical properties of materials and its low crystallization strongly affects the industrial production. Therefore, controlling the crystallization growth rate and tailoring the proportion of different polymorphs are extremely important for iPB application [5].

As is well known, the most effective method to accelerate the crystallization rate and enhance the crystallization temperature is the incorporation of nucleating agent. And the nucleating agent can reduce the crystal dimension and improve the polymer's mechanical properties. Nucleating agent is suitable for semi-crystalline polyolefin polymers, such as PE and iPP.

The nucleating agent used for isotactic polypropylene can be divided into α nucleating agents [6,7] and β nucleating agents [8-11], in which α nucleating agents can improve the tensile and flexural properties as well as transparency of iPP while β nucleating agents

can improve the impact strength and heat distortion temperature of iPP [12,13]. However few reports have focused on the correlative work of nucleating agent for iPB. Liu et al [14]. studied the effect of rare earth β nucleating agents in-situ during bulk polymerization of 1-butene. The results showed that the nucleating agent could improve the crystallization temperature and shorten the crystal transformation period. Therefore, the study of the nucleating agent of iPB has important academic value and the practical significance. Since iPB and iPP are both isotactic polymers and have similar structural features, the nucleation effect of α and β nucleating agents on iPB has been studied, meanwhile new nucleating agent which similar to TMB-5 (β nucleating agents). The new nucleating agent can be increased the crystallization temperature and crystallization rate significantly compared to pure iPB.

In this paper, we synthesized a new nucleating agent 9,10-dihydro-9,10-ethano-anthracene-11,12-dicarboxylic acid disodium salt (DHEAS) and researched its nucleation effect on poly(1-butene). The crystallization behavior was explored by differential scanning calorimetry analysis and polarized optical microscope analysis under isothermal conditions. The aims of this work are to disclose the influence of different nucleating agents on the crystallization behavior of poly(1-butene).

EXPERIMENTAL

Material
Nucleating agents: NA-21 (Asahi Denka); 68L(Milliken); rare earths (Guangdong Winner New Materials Technology Co, Ltd); aluminum p-tert-butylbenzoate and TMB-5 (Shanxi Chemical Research Institute). Anthracene and maleic anhydride (Aladdin, China). Poly(1-butene) was synthesized by our group (M_w = 45.5 kg/mol; PDI= 2.7; Isotactic degree= 98.9).

Synthesis of the new nucleating agent
Synthesis of 9,10-dihydro-9,10-ethano-anthracene-11,12-dicarboxylic acid-anhydride[15]
Anthracene (20 g, 112 mmol) and CH_2Cl_2 (250 ml) were added to a 500 ml single-necked flask and stirred in an ice-water bath. Anhydrous aluminum chloride (16.5 g, 124 mmol) was added portion-wise to this flask. A CH_2Cl_2 solution of maleic anhydride (11g, 112 mmol) was added in portions to maintain the reaction

mixture at 0°C. After warming to room temperature and stirring overnight, the suspension was carefully poured into water, the organic layer separated, and the aqueous layer extracted with CH_2Cl_2 (3×50 ml). The organic extracts were combined, washed with water and dried over $MgSO_4$, and to remove the solvent, the sample was dried in a vacuum oven to obtain a tan solid. 1H NMR (400 MHZ, DMSO-D6): δ7.54(dd, 2H) 7.39 (dd, 2H), 7.24 (m, 4H) 4.93 (s, 2H), 3.71 (s, 2H); ATR-FTIR (cm^{-1}): 2968, 1861, 1776, 1597, 1455, 1324, 1230, 1205, 1063, 975, 913, 891.

Synthesis of 9,10-dihydro-9,10-ethano-anthracene-11,12-dicarboxylic acid disodium salt (DHEAS).
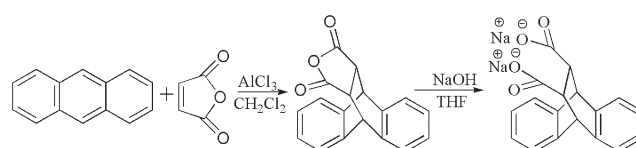9,10-Dihydro-9,10-ethano-anthracene-11,12-dicarboxylic acid-anhydride (10 g, 36 mmol) and tetrahydrofuran (250 ml) were added to a 500 ml single-necked flask. 0.1 M sodium hydroxide aqueous solution (72 mmol) was added to the flask and stirred 2 h at room temperature to concentrate and then the concentrated solution was recrystallized to obtain a white solid. ATR-FTIR (cm^{-1}): 2930, 1654, 1576, 1559, 1450, 1405, 1402, 1332, 1292,1210, 1035,848. The synthetic route of the new nucleating agent (DHEAS) is shown in Scheme 1.

Preparation of iPB samples
iPB/nucleating agent compounds were prepared by the direct melt mixing of nucleating agent with iPB in a Model Cs-163MMX at 180°C for 4min. The nucleating agent and antioxidants contents were 0.5 wt%.

Differential scanning calorimetry analysis
Differential scanning calorimetry (DSC) measurements were carried by using a TA instruments Q2000 differential scanning calorimeter. All operations were carried out under nitrogen atmosphere. The heating rate was 10°C min^{-1} ranging from 40°C to 180°C, held in the molten state for 5 min to erase their thermal history, then cooled down to 40°C at rate 10°C/min, held at 40°C for 5 min, and then finally heated again to

Scheme 1. Synthesis of the new nucleating agent.

180 °C at rate 10°C/min. The isothermal crystallization tests were performed as follows: the samples were heated to 180°C at rate 20°C/min and held in the molten state for 5 min to erase their thermal history. The sample melts were subsequently rapidly cooled to the predetermined crystallization temperature T_c and maintained at this temperature until the crystallization of the matrix was completed, and then finally heated again to 180°C at a rate of 10°C/min.

Polarized optical microscope analysis
Polarizing optical microscopy was performed using an Olympus BX51 microscope equipped with a Linkam Gray hot-stage and photo camera. Samples were sandwiched between microscope cover glasses, melted at 180°C for 5min, and then rapidly cooled to the predetermined crystallization temperature T_c to crystallize isothermally for 10 min. Photomicrographs of growing spherulites were captured at appropriate time intervals.

RESULTS AND DISCUSSION

Differential scanning calorimetry analysis
DSC, a conventional and powerful technique to study the crystallization of polymer materials [16-18], was used in our work. Firstly, the poly(1-butene) samples were prepared by the melting blend of iPB and different nucleating agents. Then the melting and crystallization processes of iPB/nucleating agents samples were studied by DSC. The melting curves and crystallization curves of iPB with different nucleating agent are presented in Figure 1. As shown in Figure
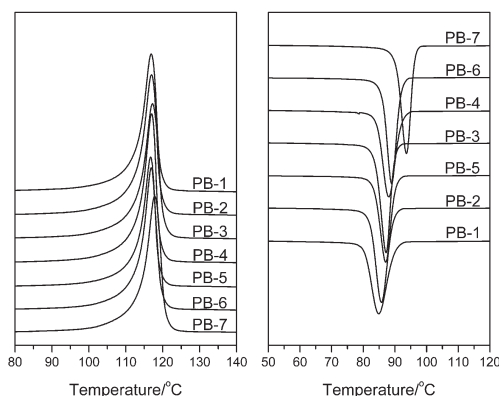
Table 1. DSC results of iPB samples with different nucleating agents.

Sample	Nucleating agent	T_c(°C)	T_m(°C)	ΔH(J/g)	X_c(%)
PB-1	-	85.0	116.8	40.5	65.3
PB-2	68L	85.8	117.0	41.9	67.5
PB-3	NA21	87.2	117.2	42.4	68.4
PB-4	Aluminum p-tert-butyl benzoate	88.2	117.0	40.7	65.7
PB-5	Rare earth	87.1	116.7	35.8	57.8
PB-6	TMB-5	89.0	116.9	40.0	64.5
PB-7	DHEAS	93.6	117.8	41.6	67.2

1, compared with the non-nucleated system PB-1, the exothermic traces of iPB samples having nucleating agent are shifted to higher temperatures as a result of nucleating agent filling, but the melting point does not show a clear change. The improved crystallization temperature indicates that the different nucleating agents are beneficial to promoting the crystallization of iPB sample. The detailed results of DSC curve are presented in Table 1. The crystallization temperature of iPB having 9,10 -dihydro-9,10-ethano-anthracene-11,12-dicarboxylic acid disodium salt (DHEAS) is higher than that of iPB with no nucleating agent and the other nucleating agents, and the crystallization temperature of iPB is up to 93.6 °C, suggesting that the DHEAS has a great nucleating effect on poly(1-butene). The other nucleating agents are also very effective nucleating agents for polypropylene, but their nucleating effect on iPB is weak, indicating that the nucleation mechanism of iPB may be different from that of PP. From Table 1, we can also see that the melting temperature and melting enthalpy for the iPB/nucleating agents samples have not changed much relative to pure iPB.

Isothermal crystallization
According to the Hoffman theory of nucleation [19,20] and Hoffman-Weeks [19] extrapolation, the melting point increases linearly with the increase of crystallization temperature. The equilibrium melting point T_m^o can be determined according to the Hoffman-Weeks equation:

$$T_m = \frac{T_c}{2\beta} + T_m^o(1 - \frac{1}{2\beta}) \tag{1}$$

where, T_m is the observed melting temperature, T_c is the selected crystallization temperature, T_m^o is the equilibrium melting point, β is a factor depending

Figure 1. DSC melting and crystallization curves of iPB sample with different nucleating agents.

Table 2. Value of the equilibrium melting temperature T_m^o and the ratio of thickness.

Sample	T_m^o(°C)	β
PB-1	121.9	3.0
PB-2	125.7	1.8
PB-6	125.2	1.8
PB-7	124.1	2.1

on the final laminar thickness, which indicates the ratio of the thickness of the mature crystal L_c to that of the initial one L_c^* [21]. The values of T_c^o can be obtained by extrapolating the least-squares fitted lines of experimental data according to Equation (1) to intersect the line of $T_m = T_c$. The value of T_m^o and β for all studied samples are listed in Table 2. It can be seen that the T_m^o of iPB /nucleating agent sample is higher than the T_m^o of pure iPB, and the β of iPB /nucleating agent sample is lower than the β of pure iPB. All these show that the nucleating agent can increase the equilibrium melting point of iPB. Because the equilibrium melting point is related to the crystal form.

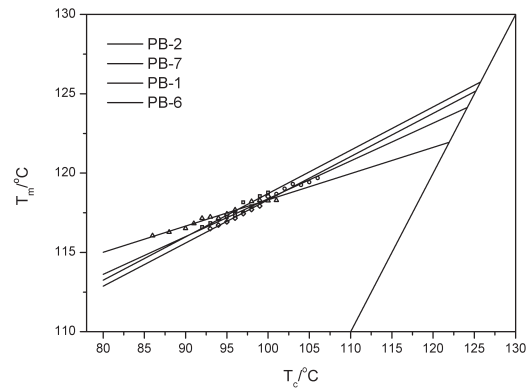Figure 3 illustrates the development of the relative

Figure 2. Hoffman-Weeks plots for determination of the equilibrium melting temperature, take PB-1, PB-2, PB-6 and PB-7 as example.

crystallinity with time for isothermal crystallization. The relative crystallinity (X_t) can be obtained from the isothermal crystallization exotherms according to the following equation [22,23]:

$$X_t = \frac{X_t(t)}{X_t(\infty)} = \frac{\int_0^t (\frac{dH}{dt})dt}{\int_o^\infty (\frac{dH}{dt})dt} \qquad (2)$$
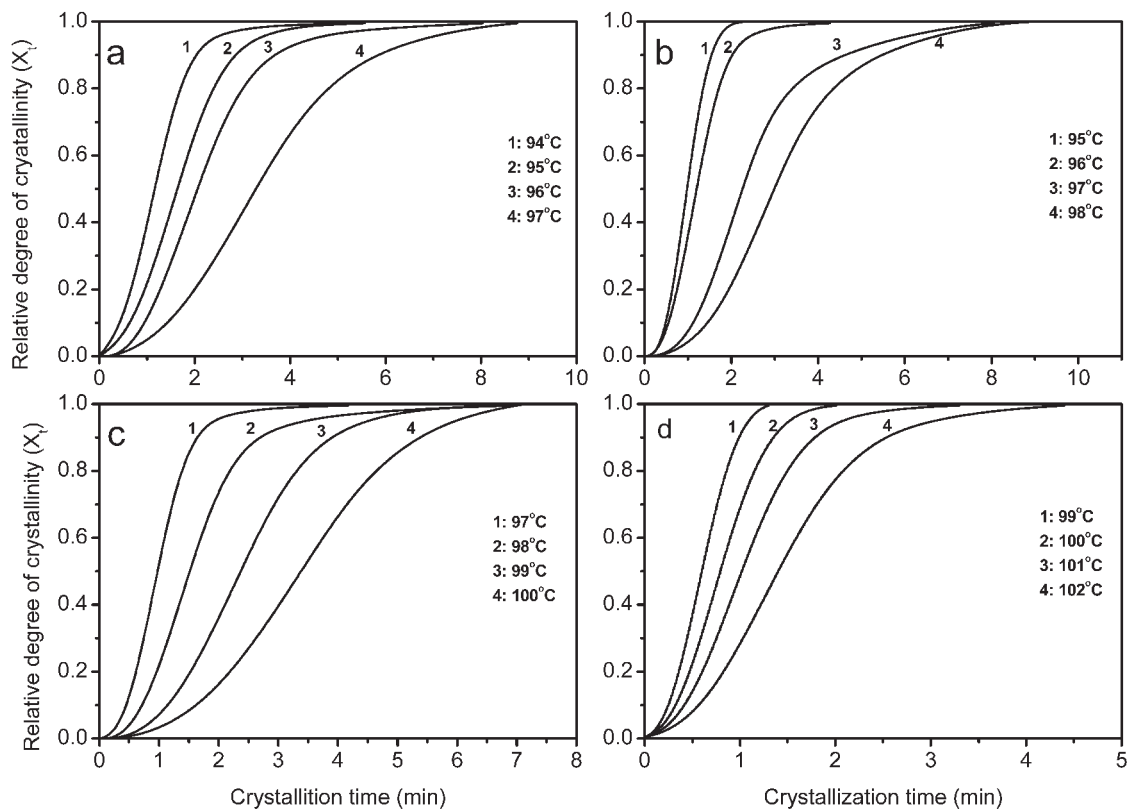

Figure 3. Development of the relative crystallinity with time for isothermal crystallization of (a) PB-1; (b) PB-2 (68L); (c) PB-6(TMB-5); (d) PB-7(DHEAS).
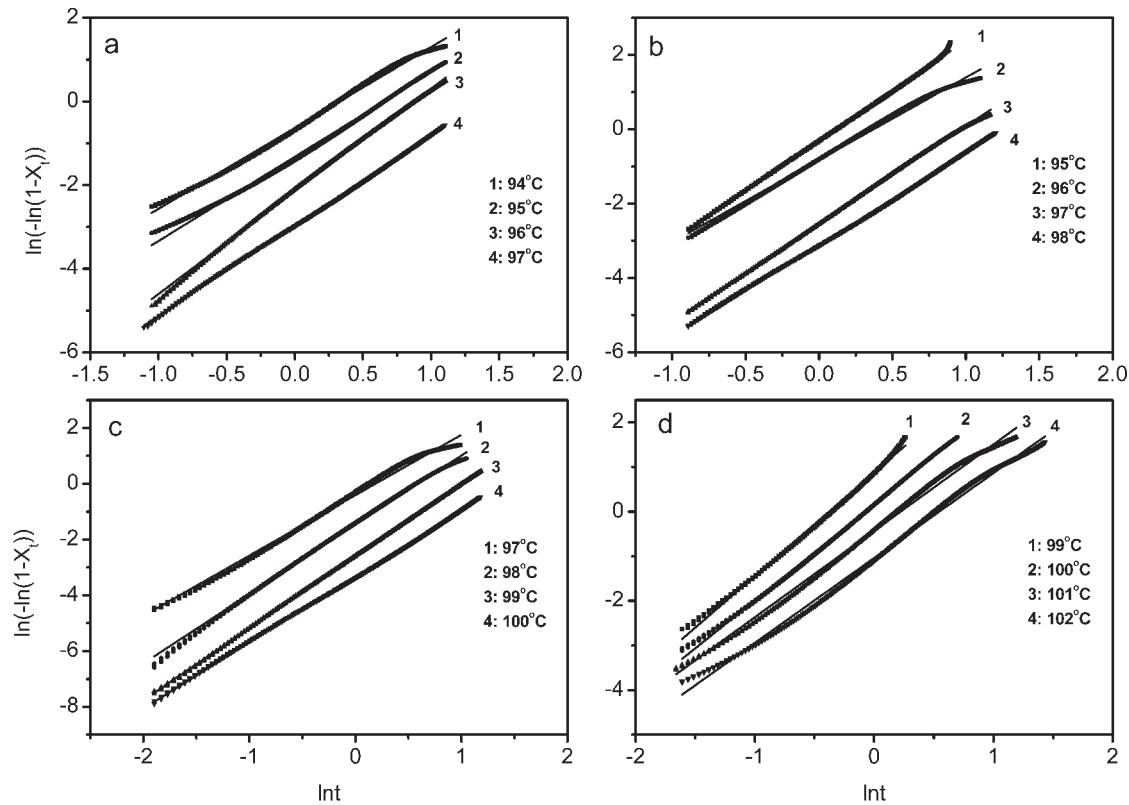
Figure 4. Avrami plots of (a) PB-1; (b) PB-2 (68L); (c) PB-6(TMB-5); (d) PB-7(DHEAS).

where, (dH/dt) is the rate of heat evolution, $X_t(t)$ and $X_t(\infty)$ represent the absolute crystallinity at time t and at the termination of the crystallization process, respectively. The plot of X_t versus t shifts to the right with increasing the crystallization temperature, which shows that the crystallization rate is enhanced as the temperature decreases, suggesting the crystallization temperature have a large effect on the relative crystallinity.

The crystallization kinetics of polymers under isothermal conditions for various modes of nucleation and growth can be well approximated by the known Avrami equation [24,25]:

$$X_t = 1 - \exp(-kt^n) \qquad (3)$$

The values of *n* and *k* are calculated from fitting to experimental data using the natural logarithm form of Equation 3.

$$\ln(-\ln(1 - X_t)) = \ln k + n \ln t \qquad (4)$$

where, the Avrami exponent (*n*) is a constant that depends on the nucleation and growth mechanism of the crystals; *k* is the crystallization rate constant involving both nucleation and growth rate parameters

under isothermal conditions.

Plots of $\ln(-\ln(1-X_t))$ vs lnt at given temperature for pure iPB and iPB with different nucleating agents are shown in Figure 4. According to Eq. 4, the values of lnk and n are obtained from the slope and the intersection of the Avrami plots. The results are listed in Table 3.

Table 3. The kinetic parameters of pure iPB and iPB with different nucleating agents.

Sample	T_c (°C)	n	lnk	k	$t_{1/2}$(min)	$\bar{n}$
PB-1	94	1.93	-0.63	0.53	1.15	2.13
	95	2.01	-1.32	0.27	1.61	
	96	2.46	-2.15	0.12	2.07	
	97	2.15	-2.98	0.05	3.36	
PB-2	95	2.67	-0.31	0.73	0.98	2.49
	96	2.21	-0.82	0.44	1.23	
	97	2.62	-2.54	0.08	2.29	
	98	2.47	-3.11	0.04	3.03	
PB-6	97	2.17	-0.41	0.67	1.02	2.40
	98	2.49	-1.47	0.23	1.56	
	99	2.58	-2.59	0.07	2.37	
	100	2.36	-3.34	0.04	3.52	
PB-7	99	2.31	0.88	2.40	0.58	2.08
	100	2.16	0.17	1.18	0.78	
	101	1.94	-0.43	0.65	1.03	
	102	1.90	1.04	0.35	1.42	

The Avrami exponent for pure iPB was found to be 2.13. The Avrami for iPB with different nucleating agents was found in the range of 2.08-2.49. The fact that the Avrami exponent is different for the pristine polymer and the iPB with different nucleating agent clearly indicates that the basic mechanism of phase transformation is altered in the presence of nucleating agent [26]. The values of the crystallization rate parameter decrease with increasing crystallization temperature, which means a decrease in the nucleation rate constant. The crystallization rate parameter of iPB/nucleating agent samples is higher than that of pure iPB at the same crystallization

temperature, which suggests the nucleating agent can accelerate the nucleation rate. In order to directly study the crystallization rate of iPB, we introduce the crystallization half-time. Crystallization half-time ($t_{1/2}$) is defined as the time at which the extent of crystallization reaches 50% [27,28]. Crystallization half-time ($t_{1/2}$) can be obtained by Eq. 5:

$$t_{1/2} = (\frac{\ln 2}{k})^{1/n} \qquad (5)$$

with the increase of the crystallization temperature, crystallization half-time ($t_{1/2}$) gradually increases. In all case, the $t_{1/2}$ of the iPB with DHEAS is shorter than
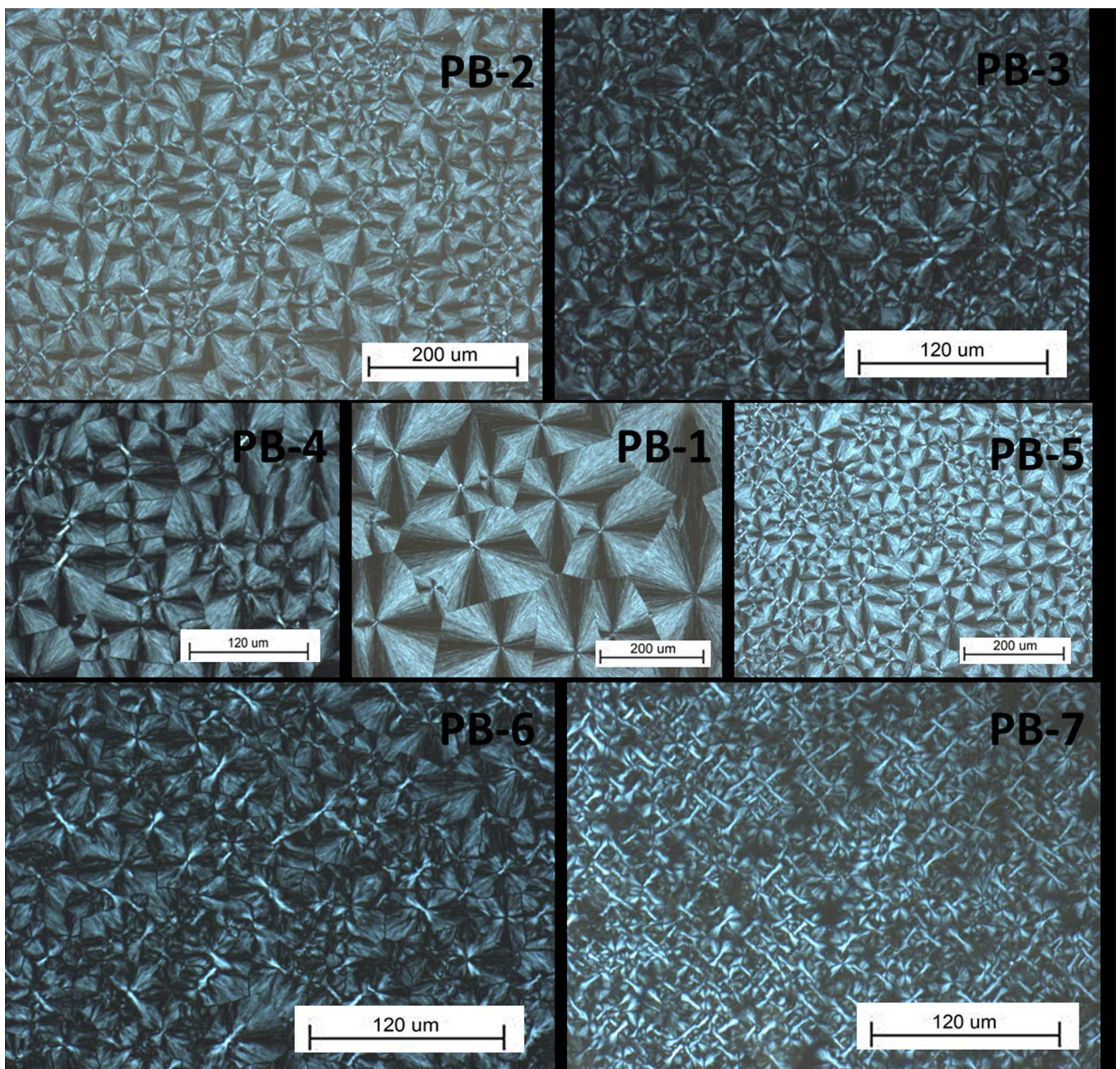

Figure 5. POM images of pure iPB and iPB with different nucleating agents.
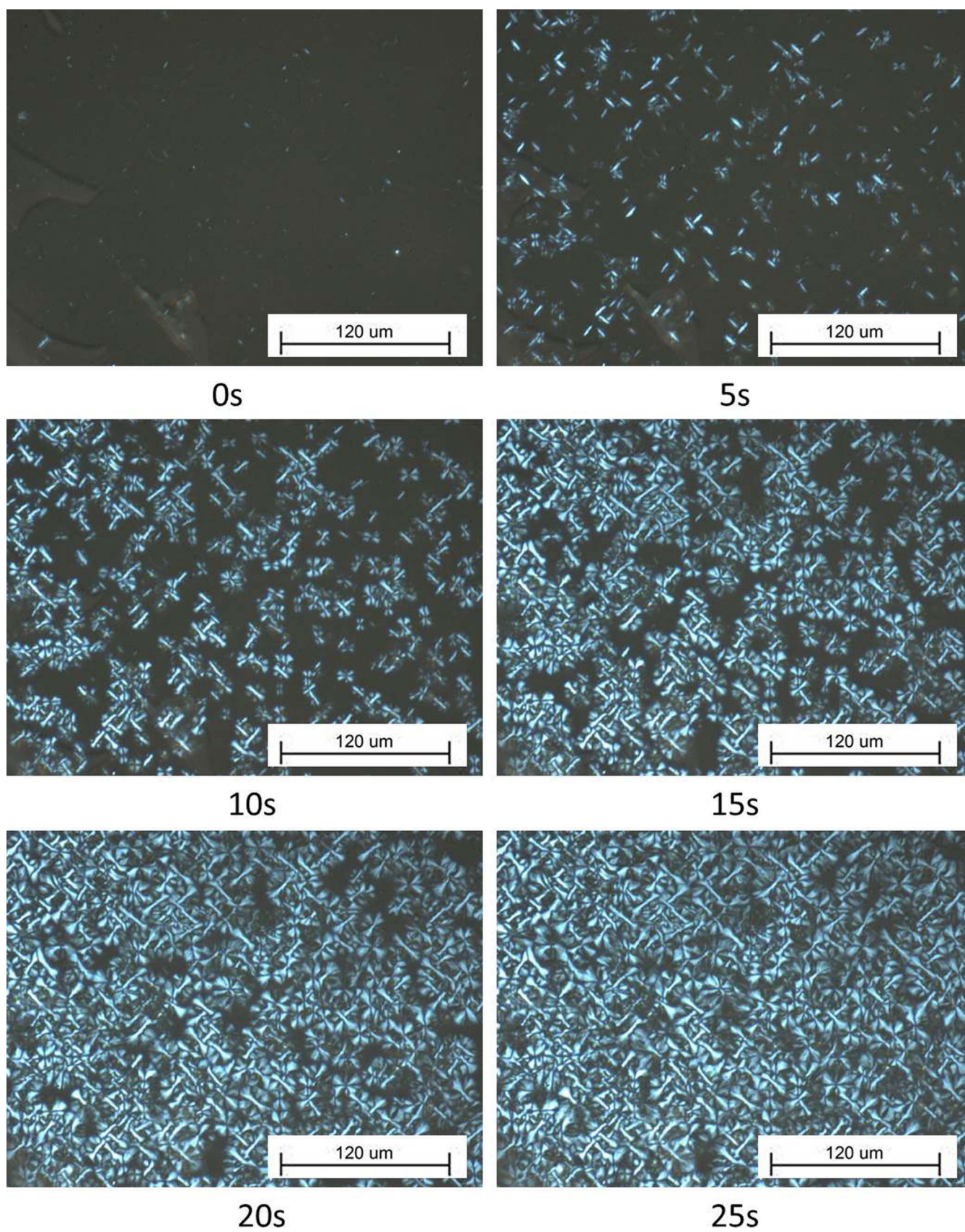
Figure 6. Evolution of the crystalline morphology during isothermeral cryatallization with time at 95°C for iPB with DHEAS.

that of the other samples. The $t_{1/2}$ of the iPB containing DHEAS is 0.58 min when the crystallization temperature is 99°C, which suggests that DHEAS can increase the crystallization rate and effectively promote the crystallization of iPB.

Polarized Optical Microscopy (POM) Analysis
The spherulitic size and morphological behavior of pure iPB and iPB with different nucleating agents were studied by a polarized optical microscope (POM) at 85°C. As shown in Figure 5, the spherulitic sizes of pure iPB are larger than those of the other iPBs, which suggests that the nucleating agent can be used as heterogeneous nuclei in the iPB matrix and can decrease the size of iPB effectively. The iPB samples possess the typical black cross extinction phenomenon exception PB-7. When DHEAS was used as nucleating agent, the spherulitic size of iPB was the smallest and the morphology was changed.

The morphology development during the isothermal crystallization of iPB with DHEAS nucleating agent at 95°C is shown in Figure 6. Clearly, the presence of DHEAS in the iPB matrix significantly influences the crystallization process and morphology of iPB. Firstly, the introduction of DHEAS into the iPB sample can promote the crystallization of iPB and shorten the crystallization time, which is consistent with the DSC results. Secondly, the addition of DHEAS leads to a substantial decrease in the spherulite size of iPB. Furthermore, the boundaries of spherulites are hardly distinguished. The phenomenon suggests DHEAS has a better nucleation effect on iPB.

CONCLUSION

In this study, we synthesized a novel nucleating agent for iPB, and researched the influence of different nucleating agents on the isothermal crystallization of iPB. The addition of the nucleating agent into iPB could enhance the crystallization temperature, and the crystallization temperature of iPB with DHEAS was 9°C higher than that of pure iPB. The isothermal crystallization kinetics results showed that the addition of nucleating agent accelerated the crystallization rate and decreased the crystallization half-time. Compared with α-nucleating agent and β-nucleating agent, iPB nucleated with DHEAS had smaller crystallization half-time at higher temperature than virgin iPB at

lower crystallization. In addition, incorporation of nucleating agent DHEAS could decrease the spherulite size of iPB and dramatically shortened the crystallization time. Therefore, the novel nucleating agent DHEAS has better nucleation effects on iPB.

REFERENCES

1. Gonzalez I, Eguiazabal J, Nazabal J (2005) Compatibilization level effects on the structure and mechanical properties of rubber modified polyamide 6/clay nanocomposites. J Polym Sci B: Polym Phys 43: 3611-3620
2. Huang J, Keskkula H, Paul D (2006) Comparison of the toughening behavior of nylon 6 versus an amorphous polyamide using various maleated elastomers. Polymer 47: 639-651
3. Chen X, Yu J, Luo Z, Guo S, He M, Zhou Z (2011) Study on mechanical properties and phase morphology of polypropylene/polyolefin elastomer/magnesium hydroxide ternary composites. Polym Adv Technol 22: 657-663
4. Qiu G, Liu G, Qiu W, Liu S (2013) Phase morphology and mechanical properties of polyamide-6/ polyolefin elastomer- g - maleic anhydride blends. J Macromol Sci, B 53: 615-624
5. Choi M, Jung J-Y, Chang Y-W (2014) Shape memory thermoplastic elastomer from maleated polyolefin elastomer and nylon 12 blends. Polym Bull 71: 625-635
6. Nishitani Y, Yamada Y, Ishii C, Sekiguchi I, Kitano T (2010) Effects of addition of functionalized SEBS on rheological, mechanical, and tribological properties of polyamide 6 nanocomposites. Polym Eng Sci 50: 100-112
7. Isik-gulsac I, Yilmazer U, Bayram G (2013) Effects of addition order of the components on polyamide-6/ organoclay/ elastomer ternary nanocomposites. Adv Polym Technol 32: E675-E691
8. Kohan MI, Kohan MI (1995). Nylon plastics handbook, Hanser Publishers

9. Lincoln DM, Vaia RA, Wang ZG, Hsiao BS (2001) Secondary structure and elevated temperature crystallite morphology of nylon-6/layered silicate nanocomposites. Polymer 42: 1621-1631

10. Maiti P, Okamoto M (2003) Crystallization controlled by silicate surfaces in nylon 6 clay nanocomposites. Macromol Mater Eng 288: 440-445

11. Li TC, Ma J, Wang M, Tjiu WC, Liu T, Huang W (2007) Effect of clay addition on the morphology and thermal behavior of polyamide 6. J Appl Polym Sci 103: 1191-1199

12. Liu X,Wu Q (2002) Phase transition in nylon 6/ clay nanocomposites on annealing. Polymer 43: 1933-1936

13. Wu TM, Liao CS (2000) Polymorphism in nylon 6/clay nanocomposites. Macromol Chem Phys 201: 2820-2825

14. Cui L,Yeh JT (2010) Nylon 6 crystal phase transition in nylon 6/clay/poly (vinyl alcohol) nanocomposites. J Appl Polym Sci 118: 1683-1690

15. Chiu FC, Lai SM, Chen YL, Lee TH (2005) Investigation on the polyamide 6/organoclay nanocomposites with or without a maleated polyolefin elastomer as a toughener. Polymer 46: 11600-11609

16. Lee KM, Han CD (2003) Rheology of organoclay nanocomposites: Effects of polymer matrix/ organoclay compatibility and the gallery distance of organoclay. Macromolecules 36: 7165-7178

17. Xie W, Gao Z, Pan W-P, Hunter D, Singh A, Vaia R (2001) Thermal degradation chemistry of alkyl quaternary ammonium montmorillonite. Chem Mater 13: 2979-2990

18. Brandrup J (1989) Polymer Handbook. 3rd ed. John Wiley and Sons, New York

19. Paci M, Filippi S, Magagnini P (2010) Nanostructure development in nylon 6-Cloisite® 30B composites. Effects of the preparation conditions. Eur Polym J 46: 838-853

20. Gomari S, Ghasemi I, Karrabi M, Azizi H (2012) Organoclay localization in polyamide 6/ethylene-butene copolymer grafted maleic anhydride blends: The effect of different types of organoclay. J Polym Res 19: 1-11

21. Ying JR, Liu SP, Guo F, Zhou XP, Xie XL (2008) Non-isothermal crystallization and crystalline structure of PP/POE blends. J Therm Anal Calorim 91: 723-731

22. Benderly D, Siegmann A, Narkis M (1997) Structure and behavior of multicomponent immiscible polymer blends. J Polym Eng 17: 461-490

23. Zhang L, Wan C, Zhang Y (2008) Polyamide 6/ maleated ethylene - propylene - diene rubber/ organoclay composites with or without glycidyl methacrylate as a compatibilizer. J Appl Polym Sci 110: 1870-1879

24. Katoh Y, Okamoto M (2009) Crystallization controlled by layered silicates in nylon 6–clay nano-composite. Polymer 50: 4718-4726

25. Wang B, Hao L, Wang W, Hu G (2009) One-step compatibilization of polyamide 6/poly (ethylene-1-octene) blends with maleic anhydride and peroxide. J Polym Res 17: 821-826

26. Wahit M, Hassan A, Mohd Ishak Z, Czigány T (2009) Ethylene-octene copolymer (POE) toughened polyamide 6/ polypropylene nanocomposites: Effect of POE maleation. Express Polym Lett 3: 309-319

27. Cervantes-Uc JM, Cauich-Rodríguez JV, Vázquez-Torres H, Garfias-Mesías LF, Paul DR (2007) Thermal degradation of commercially available organoclays studied by TGA–FTIR. Thermochim Acta 457: 92-102